Journal of Structural Geology, Vol. 1, No. 3, 1979, pp. 187 to 205.

Geometry of crenulation-folds and their relationship to crenulation cleavage

DAVID R. GRAY

Department of Geological Sciences, Virginia Polytechnic Institute and State University, 4044 Derring Hall, Blacksburg, VA 24061, U.S.A.

(*Received* 7 *March* 1979; *accepted in revised form* 22 *August* 1979)

Abstract—Analysis and descriptions of the geometry and wavelengths of crenulation-folds from crenulated, low grade metamorphic rocks from southeastern Australia are related to existing theoretical and experimental work on folding. Isogon line behaviour and shape contrasts of the folds indicate that the pre-existing anisotropy in these rocks has been mechanically active during the crenulation deformation. Fabric parameters such as grainsize and proportions of flaky minerals (statistically homogeneous fabrics), and layer thickness and layer rheology contrast (multilayer fabrics), markedly influence the wavelengths of the crenulation-folds. These features are incompatible with passive-slip folding and support a buckling origin. Relationships between crenulation cleavages and these folds suggest that the cleavages are associated with two types of buckling instabilities. The most common association (Type A instability) is internal buckling within a confined anisotropic medium, whereas the other (Type B instability) relates to micro-buckling in the contact strain zone adjacent to buckled competent 'single layers'. Amplification and propagation of both instability types will produce folds which become potential sites for differentiation processes to operate to produce cleavages. The crenulation-folds are therefore a necessary pre-requisite for development of crenulation cleavages. They determine the location, the spacing and the lengths of crenulation cleavages in crenulated anisotropic fabrics. They do not however influence the variety of crenulation cleavage which develops since there is no apparent relationship between cleavage type and a particular fold geometry.

INTRODUCTION

FOLDS associated with crenulation cleavages in poly-deformed metamorphic rocks are referred to here as crenulation-folds. They are characterized by an axial plane crenulation cleavage and range from mesoscopic folds observable in outcrop, to microfolds. The microfolds, better known as crenulations (Rickard 1966), are harmonic and typically of short wavelength (generally less than a few cm) with sub-sinusoidal forms. They have an almost ubiquitous association with both the discrete and zonal varieties of crenulation cleavage (Gray 1976, 1979). This association has long been recognized (cf. Heim 1878, Dale 1892, White 1949, Rickard 1961), but little is known about crenulation-folds, in particular the factors which determine their formation and their final geometry.

Earlier work on crenulation-folds (cf. Hills 1945, Campbell 1951, De Sitter 1954, 1956, Donath & Parker 1964) suggested they were passive-slip folds (Donath & Parker 1964) resulting from slip along the cleavage planes. This implied (i) passive layer behaviour during folding, and (ii) that the fold geometry was determined by the movements along the cleavage. Observed offsets in veins and layering along discrete crenulation cleavages, and a somewhat 'similar' (class 2) geometry for many crenulation-folds, were cited as evidence to support this. Two hypotheses, firstly heterogeneous simple shear acting parallel to the fold axial surfaces, the 'classical' explanation, and secondly differential flattening producing differential shear (Ramsay 1962) were proposed to explain the mechanics of passive folding. Arguments against both hypotheses have been put forward (see Flinn 1962, p. 425, Mukhopadyay 1965, Hudleston 1973a, p. 27, 1973b, p. 120). Furthermore, there is no real evidence of significant movement, that is movement over several centimetres, along crenulation cleavages. The observed offsets of markers along discrete types are only apparent and can be explained by local volume reductions along the cleavages (Durney 1972, Gray 1977a, 1979).

More recent investigations to determine the mechanics of formation of crenulation-folds have been made indirectly through theoretical and experimental studies of multilayer folding (Ramberg 1960, 1962, 1963a, 1964, 1970, Biot 1960, 1963, 1964, 1965, 1967, Ghosh 1968, Bayly 1970, 1971, 1974, Cobbold *et al.* 1970, Johnson 1970, 1977, Cosgrove 1972, 1976, Cobbold 1976). Most of the theoretical work considers that crenulations develop from buckling-instabilities in anisotropic media, where their final geometry is dependent on variables of the medium such as the type of fabric layering and its degree of anisotropy, the orientation of the anisotropy with respect to the principal stress axes, and the degree of crenulation development (see Cosgrove 1976, pp. 176–177). This implies that the pre-existing anisotropy plays an 'active' role in the development of crenulation-folds.

At present data on natural crenulation-folds enabling correlation with theoretical and experimental work is lacking. The object of this paper is to provide such data, and to attempt to determine the genesis of crenulation-folds by examination of their geometry and associated features. The folds analyzed occur in poly-deformed, low to medium grade regionally metamorphosed rocks from the southeastern part of the Palaeozoic Tasman Structural Province, Australia (see Rutland 1976, fig. 1). It is emphasized that the folds and their associated

crenulation cleavages are distinctly similar to those in rocks of equivalent metamorphic grade from other continents (see Gray 1979, p. 97). The analyses and discussion in this paper should therefore have general applicability. The morphology, microstructure and suggested origin for the crenulation cleavages are discussed elsewhere (see Gray 1976, 1977a, 1979).

An attempt is made here to determine firstly, those parameters which influence crenulation-fold shape and wavelength, and secondly, how folding influences the propagation of crenulation cleavages. Aspects of crenulation-fold geometry such as shape, tightness, asymmetry and shortening are described and relationships between the folding, the cleavage spacing and cleavage length defined. Data from the descriptive and analytical sections are then used to discuss firstly, aspects of multilayer folding theory relevant to crenulation-folds, and secondly the mechanical significance of crenulation-folds.

GEOMETRY OF CRENULATION-FOLDS

The geometry of a fold is specified by attributes of the layer or surface which define the fold in the profile section; these include size, shape, tightness and asymmetry. Such geometrical features must reflect some of the following: (1) the mechanics of folding, (2) the stress states during folding, (3) the mechanical properties of the material, and possibly (4) the deformation path from the unstrained to the strained state. Analysis of the finite fold shape will not however provide precise correlations with these factors, particularly (2) and (4) (see Ramsay 1967, pp. 342 – 345, Hobbs 1971, Hudleston 1973a, p.2). This section therefore will only give a description of crenulation-fold geometry. Various analytical methods are used in an attempt to define precisely crenulation-fold morphology. Interpretation of the described fold geometry in terms of mechanics of folding is attempted in the discussion section, by analogy with folding theory and the results of folding experiments (compare Hudleston 1973b). The geometrical analyses which follow all refer to profile sections of crenulation-folds.

Fold class

Fold class is characterized by the inclinations of isogon lines (see Ramsay 1967, pp. 363–372). These lines join points of equal slope along successive surfaces of the fold profile. They may be convergent (fold class 1), parallel (fold class 2), or divergent (fold class 3). Isogon analysis of crenulation-folds (Fig. 1; also Gray 1976, figs. 4.5 and 4.6) show they commonly consist of class 1 folds, either 1B or 1C, alternating with class 3 folds. Even crenulated fabrics with overall similar fold geometry (Fig. 1d) consist of alternating class 1 and class 3 fold forms, although the deviation of isogon lines from layer to layer is less marked (compare Fig. 1a with 1d). Some individual layer-folds approach class 2 geometry, but the overall isogon pattern through the folds does not have perfect

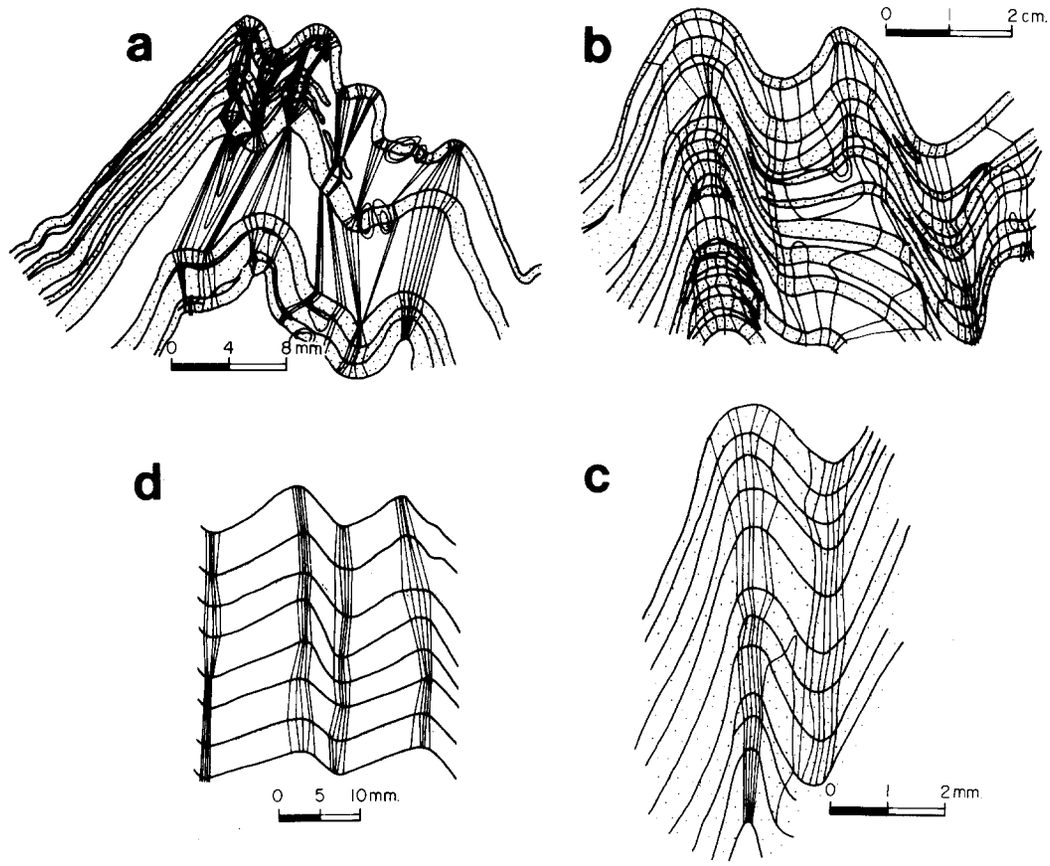

Fig. 1. Isogon patterns for selected fold types in different pre-existing fabrics. The isogon lines are at 10° intervals. (a) Lithological layering multilayer: Gundagai, N.S.W. (MU. 10583). (b) Differentiated S_1 layering multilayer: Nambucca Heads, N.S.W. (MU. 10576). (c) Psammite multilayer: Gundagai, N.S.W. (MU. 10622). (d) Lithological layering multilayer: Captains Flat, N.S.W. (MU. 10530).

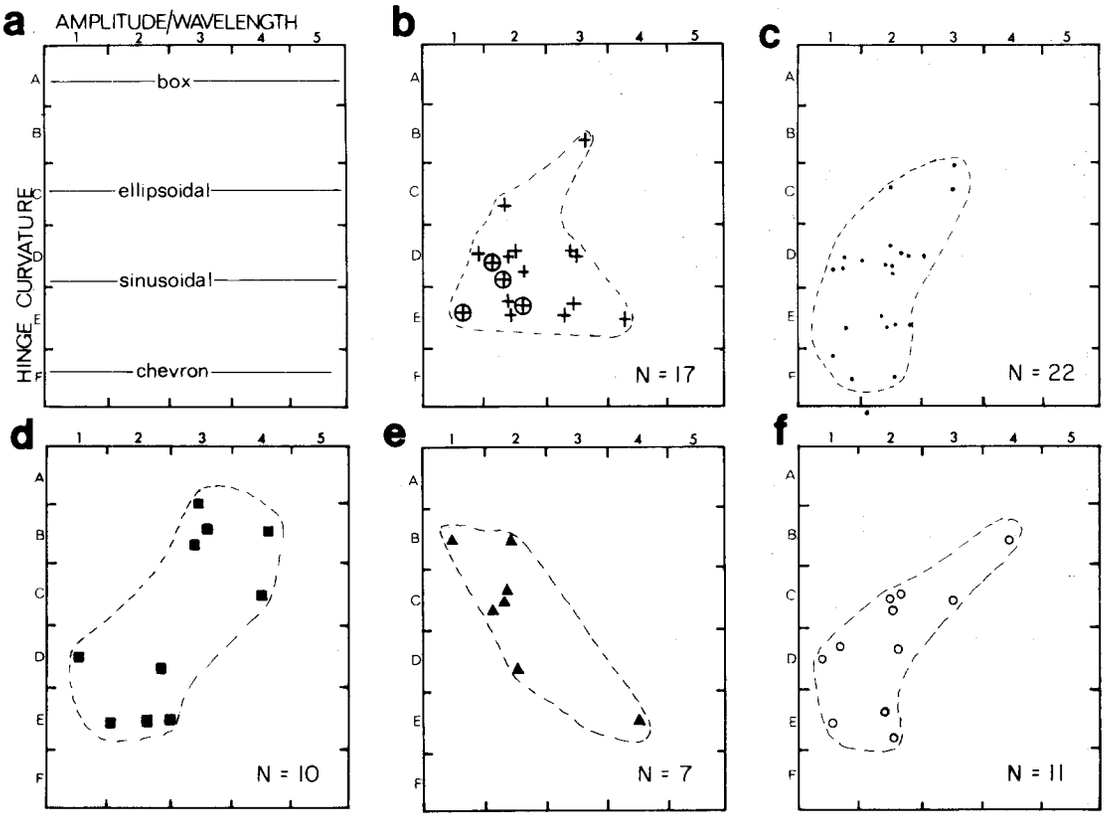

Fig. 2. Graphs after Hudleston (1973, fig. 13B) of hinge curvature ('shape') vs the ratio of amplitude/wavelength ('amplitude') for crenulation-folds in different pre-existing fabrics. (a) Fold shape positions on the Hudleston graph. (b) Slate (+) and schist fabrics (⊕). (c) Lithological layering fabrics (●). (d) Differentiated S_1 layering fabrics (■). (e) Pre-existing crenulation cleavage fabrics (▲). (f) Psammite fabrics (o).

parallelism. Figure 1 indicates that the amount of isogon line deviation reflects the nature of the pre-existing fabric anistropy. Fabrics with a distinct heterogeneous anisotropy, that is those with marked competence contrast such as between psammite and pelite layers, show maximum isogon line deviation (Fig. 1a & b), whereas those with a weak heterogeneous anisotropy, that is weak competence contrast, show minimum isogon line deviation (Fig. 1c & d).

Fold shape

This reflects the relative rates of change of inclination of the folded surface particularly at the hinge. It is specified here by 'shape' (sharpness of the hinge) and 'amplitude' (amplitude over quarter wavelength) parameters after Hudleston (1973a, figs. 12 and 13). These are determined by 'visual harmonic-analysis' (see Hudleston 1973a, pp. 24–25) of the fold form. The analysis of crenulation-fold shape (Fig. 2) shows that each particular fabric has a certain folding-association. Schist and slate fabrics (Fig. 2b) have a single point clustering which indicates a predominant sinusoidal form, whereas the lithological layering, differentiated S_1 layering, psammite fabrics and pre-existing crenulation cleavage fabric graphs define distinct linear cluster-zones – (Fig. 2c–f). The slopes of these linear zones provide information on the changes in hinge curvature of the folds. A positive slope (shown on graphs for lithological layering, differentiated S_1 layering and the psammite fabrics) indicates that the hinge curvature of these folds does not change much as they tighten, whereas a negative slope (shown on the graph for pre-existing crenulation cleavages) indicates that the hinge curvature becomes accentuated as the folds tighten. Crenulation folds, except those in slate and schist fabrics, show a variety of hinge shapes ranging from chevron to sinusoidal to ellipsoidal (see Fig. 2). There is therefore no one dominant fold shape associated with microfolds in crenulation cleavage fabrics, and the fold shape does not appear to be strongly influenced by lithology and the fabric, for the crenulation folds analyzed.

Fold tightness

Fold tightness is dependent on the size of the fold interlimb angle (cf. Fleuty 1964, p. 470). Interlimb angles of the crenulation-folds measured are mostly close, open or gentle, and range from 30° to 140°.(Fig. 3a). There is no marked dependence of fold tightness upon lithology and fabric, as shown by the diffuse pattern of Fig. 3(a).

Fold asymmetry

The ratio of the limb lengths of a fold provides a quantitative measure of the degree of asymmetry (cf. Hudleston 1973b, p. 97); symmetrical folds have an asymmetry index of 1. Crenulation-folds are commonly asymmetrical and have a range of asymmetry indices from 1.0 to 4.9 (Fig. 3b). The figure indicates that

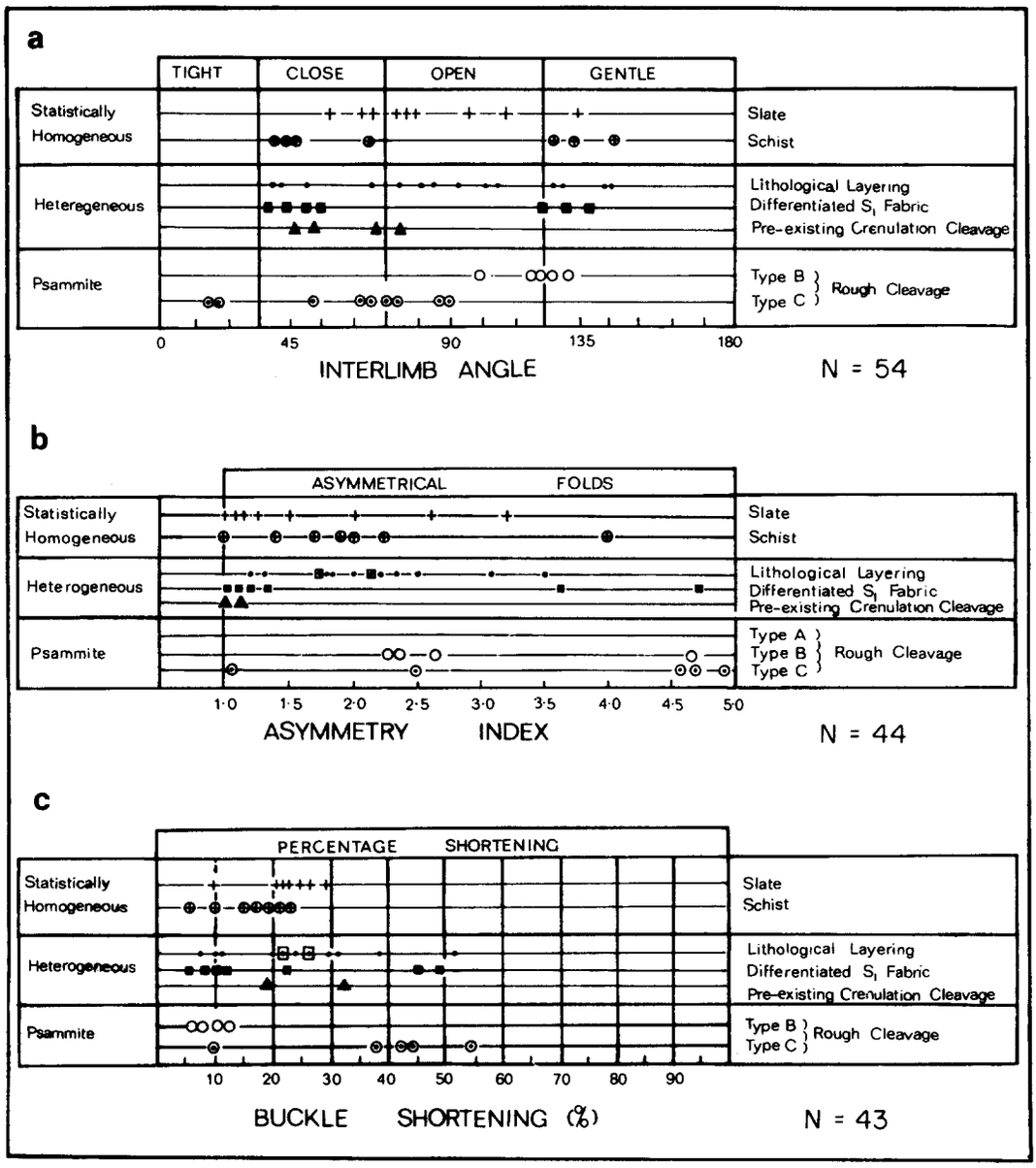

Fig. 3. Parameters of crenulation-folds (tightness, asymmetry and the amount of buckle shortening) plotted against the different pre-existing fabrics in which they occur. (a) Graph showing the degree of tightness of crenulation-folds. (b) Graph of asymmetry index of crenulation-folds. (c) Graph showing the minimum shortening values of crenulation-folds. +, slate; ⊕, schist; •, lithological layering; ■, differentiated S_1 layering; ▲, pre-existing crenulation cleavage; o, psammite with a Type B rough cleavage; ⊙, psammite with Type C rough cleavage.

degree of asymmetry varies with fabric type, although asymmetry appears to be greater in psammites than the other fabrics.

Fold shortening

Folding may involve both layer and buckle shortening (cf. Biot 1961, Ramberg 1964, Ramsay 1967, p. 379, Dieterich 1970). Values of layer shortening are difficult to determine for natural folds unless suitable markers are present in the layer (see Hudleston & Holst 1977). Because such markers are rare in crenulated fabrics only the component of buckle shortening can generally be determined. The shortening values for crenulation-folds discussed here are therefore minimum shortenings, since they do not consider layer shortening. Buckle shortening is obtained by comparing the straight line distance with the corresponding arc length measured along the layer between any two adjacent hinge points or inflexion points. Crenulation-folds have shortening values which range from 5 to 55%. The majority, 75% of those measured, have less than 30% shortening, and did not have any associated crenulation cleavage. The results suggest firstly there is no lithological control on the amount of shortening which may develop in particular fabrics, and secondly that crenulation cleavage is only associated with fabrics which have undergone at least 30% shortening.

CRENULATION–FOLD WAVELENGTH

Fold wavelength has received considerable attention in the development of mechanical theories of folding (cf. Biot 1957, 1961, 1964, 1965, Ramberg 1960, 1963, 1964, Sherwin & Chapple 1968, Johnson 1970, 1977, Hudleston 1973b, 1973c, Fletcher 1974, 1977a, Cob-

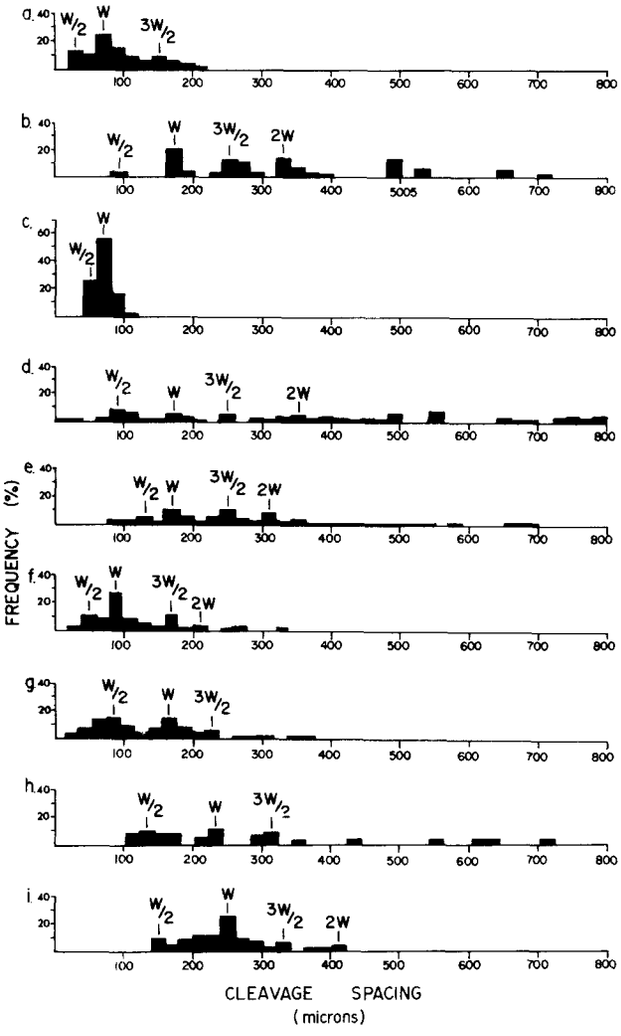

Fig. 4. Histograms of crenulation cleavage spacing in various 'unconfined' statistically homogeneous slate fabrics. The samples are arranged from (a) to (i) in order of increasing quartz grainsize. 100 measurements of cleavage spacing were taken from each sample. Histogram peaks represent some multiple of the crenulation-fold wavelength (*W*). (a) Limerick, N.S.W., MU. 10523; (b) Sofala, N.S.W., MU. 10540; (c) Greenmantle, N.S.W., MU. 10531; (d) Bermagui, N.S.W. MU. 10524; (e) Blowering Dam N.S.W., MU. 10525; (f) Torrens Gorge, S.A., MU. 10539; (g) Captains Flat, N.S.W., MU. 10533; (h) West Moruya, N.S.W., MU. 10503; (i) Broken Hill, N.S.W., MU. 10523.

bold 1975, Shimamoto & Hara 1976, Fletcher & Sherwin 1978) as it reflects or is some function of the type of folding. Theoretical treatments have shown that layer thickness, competency contrast between layers, degree of cohesion along layer interfaces, and rheology all influence fold wavelength.

Measurable features of crenulated rock fabrics such as grain size, mineral proportions and confinement distance for statistically homogeneous fabrics, and layer thickness or the multilayer thickness ratio for multilayer fabrics are correlated with the wavelengths of crenulation-folds in this section. The aim is to try and establish those fabric parameters which determine crenulation wavelength and thereby provide a basis for selection of folding-theory applicable to crenulation folds.

To facilitate the analysis, cleavage spacing rather than fold wavelength was used, because most rocks containing crenulation cleavages, particularly those with discrete types, contain a greater number of actual cleavages than crenulations. Cleavage spacing should be an indirect measure of fold wavelength, since crenulation cleavages, both discrete and zonal types, represent the former limbs of microfolds (Gray 1976, 1979). This is substantiated by an analysis of discrete cleavage spacing (Figs. 4 and 5) which shows a periodicity in spacing which is some multiple of fold wavelength in the fabrics. Comparison of peaks on both cleavage spacing and fold wavelength histograms in Fig. 5 shows that the spacing of cleavage adjacent to buckled quartz veins in a polydeformed slate (Fig. 13) correlates with the wavelength (*W*) of the buckled veins. In each case the interpreted wavelength (W_s) from the cleavage spacing is slightly less than the corresponding *W* spacing value from the vein. These deviations reflect a component of solution shortening across the cleavage related to the cleavage development. This will cause W_s to be less than *W*. The cleavage spacing histogram data of Fig. 4 have therefore been interpreted in an attempt to define the associated microfold wavelength (*W*). Each peak, as shown on the histograms, is considered some multiple of this wavelength.

Each of the following parameters are correlated with cleavage spacing.

Grain size

Graphs of grainsize vs cleavage spacing for nine crenulated pelitic mineral fabrics (Fig. 6a & b) show (1) that there are relationships between cleavage spacing, and therefore fold wavelength, and mica and quartz grainsize in these fabrics, and (2) that mica has a more important influence than quartz on cleavage spacing, and therefore fold wavelength. Different orders of cleavage spacing shown by best fit lines 1 to 4 on both graphs reflect different multiples of the dominant fold wavelength; 1 (defined by •) represents cleavages spaced at a half-wavelength ($\lambda/2$), 2 (defined by o) represents cleavages spaced at a full-wavelength (λ), 3 (defined by ■) represents $3\lambda/2$ spacing and 4 (defined by ▲) represents 2λ spacing. The best fit lines have almost identical slopes ranging from 0.42 to 0.55 for mica (Fig. 6a) and from 0.78 to 1.14 for quartz (Fig. 6b). This strongly suggests that the inferred correlation is not just coincidental. Linear regression shows a strong correlation for mica (r^2 ranges from 0.67 to 0.94 with a mean of 0.82), but a very weak correlation for quartz (r^2 ranges from 0.07 to 0.42 with a mean of 0.19). Quartz grainsize for the samples analyzed has little influence on cleavage spacing. Spacing appears strongly dependent on mica grainsize for these essentially unconfined pelitic mineral fabrics (i.e. fabrics where the pelitic layer thickness is effectively infinite with respect to the width of the micas present). The analysis indicates the relationship to a first approximation is of the form:

$$S \approx W_d = 0.49l + 160 \quad (1)$$

where S = cleavage spacing (μ), W_d = 'dominant wavelength' (μ) and l = mica length (μ). The micas in

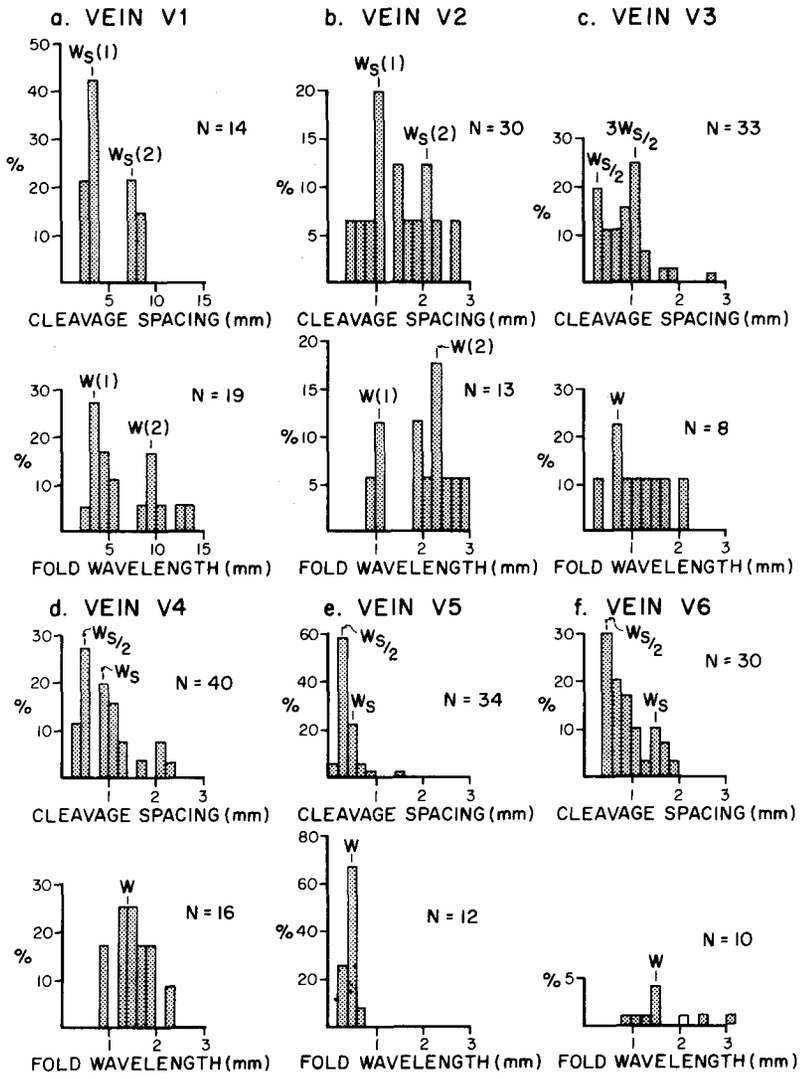

Fig. 5. Histograms of cleavage spacing (mm) and the associated fold wavelength (mm) for various buckled quartz veins in a polydeformed slate from Sofala, N.S.W. Structural relationships between the veins and the cleavage are shown in Fig. 12. Peaks on the cleavage spacing histogram are some multiple of the fold wavelength (W). Peaks on the wavelength histograms reflect the dominant wavelength (L) for the buckled veins; veins V_1 and V_2 contain two orders of folding.

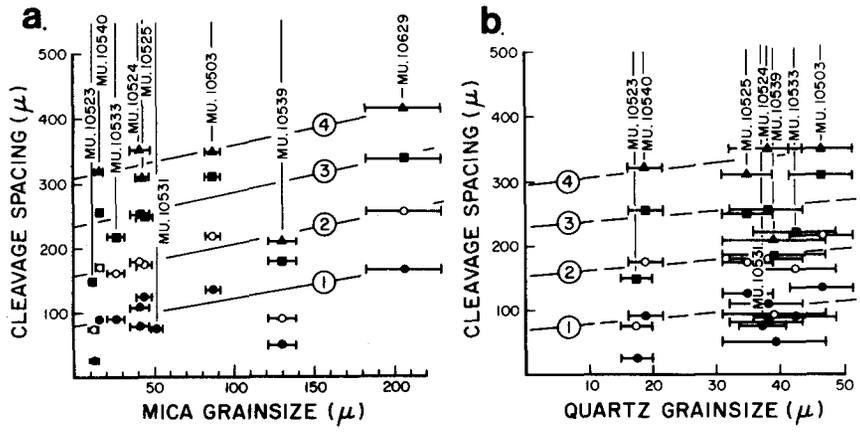

Fig. 6. Graphs of cleavage spacing (μ) vs (a) mica grainsize (μ) and (b) quartz grainsize (μ) for 'unconfined' statistically homogeneous slate and schist fabrics. Each data point represents the mean of 50 length measurements of either mica or quartz. Bar lengths indicate the standard deviation.

MU. 10523: Limerick, N.S.W. MU. 10531: Greenmantle, N.S.W.
MU. 10540: Sofala, N.S.W. MU. 10503: West Moruya, N.S.W.
MU. 10533: Captains Flat, N.S.W. MU. 10539: Torrens Gorge, S.A.
MU. 10524: Bermagui, N.S.W. MU. 10629: Broken Hill, N.S.W.
MU. 10525: Blowering Dam, N.S.W.

Best fit lines 1 (●), 2(o), 3(■) and 4(▲) reflect different orders of cleavage spacing in the fabrics. (See text)

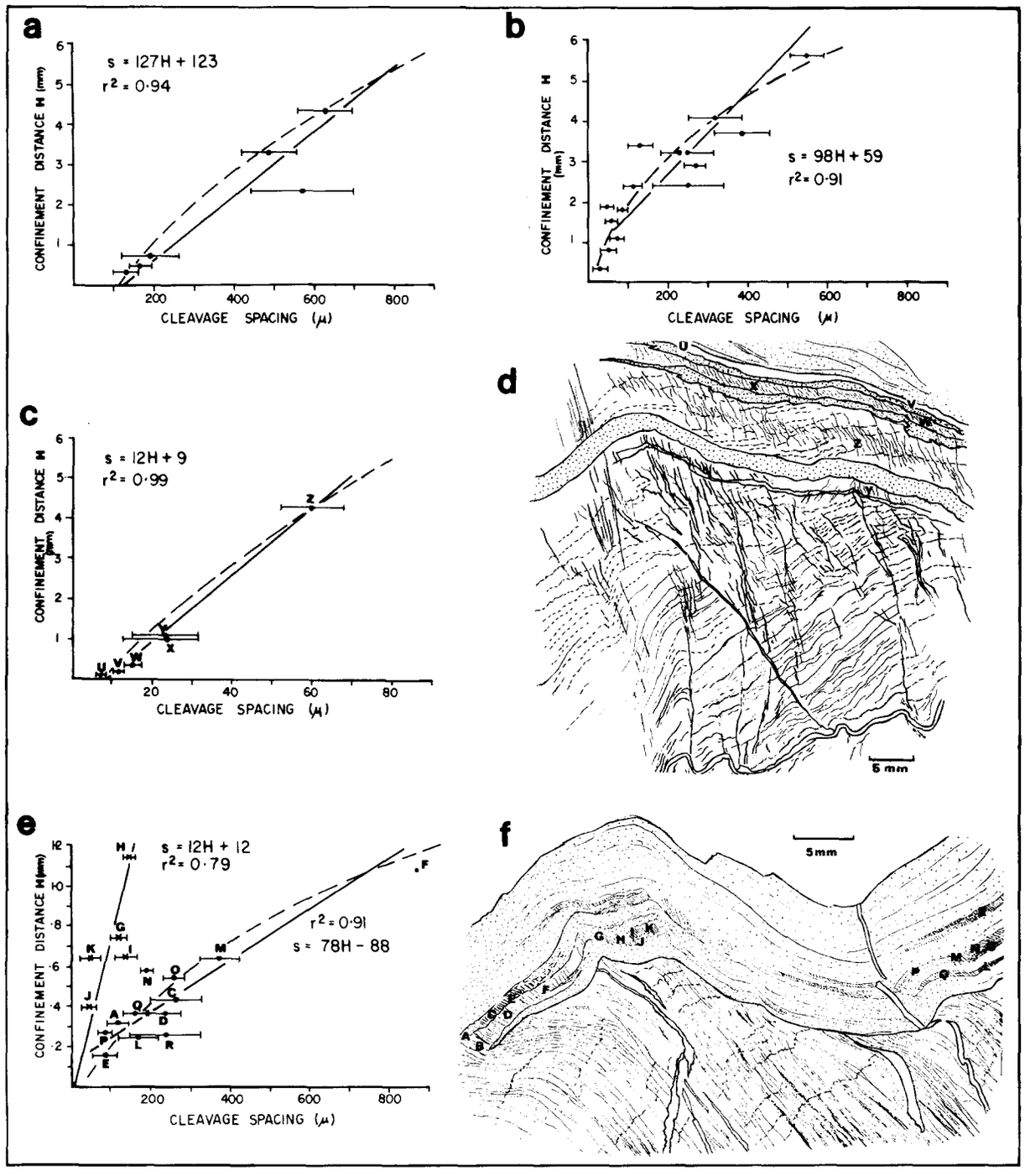

Fig. 7. Graphs of crenulation cleavage spacing (μ) vs confinement distance (mm) for a pre-existing crenulation cleavage fabric (a) and lithological layering fabrics (b, c and e). Points on each graph represent the mean of 30 – 50 cleavage spacing measurements. Bar lengths indicate the standard deviation. Fabric sketches (d) and (f) show the measurement locations for specimens (c) and (e) respectively. (a) Bermagui, N.S.W. (MU. 10537). (b) Sofala, N.S.W. (MU. 10610). (c) Blowering Dam, N.S.W. (MU. 10525). (e) West Moruya, N.S.W. (MU. 10522).

the fabrics analysed all have aspect ratios (l/w) less than 10. When fold interference occurs due to contact strain effects from closely-spaced, adjacent layers, that is the confined layer case, then the above relationship does not hold. This is shown by samples MU. 10523 and MU. 10539 (Fig. 6a) which do not fall along the lines of best fit. Both have cleavage spacing smaller than that expected for their particular mica size, a variation related to the presence of larger mesoscopic folds. Figure 7(d) shows that variations in cleavage spacing for any given layer do occur around asymmetric mesoscopic folds. Data from MU. 10523 and MU. 10539 were consequently not included in the linear regression analysis.

In contradiction to the relationships defined in Fig. 6, Potter (1968, p. 284) claims there is no direct relationship between the size of microfolds in a confined micaceous fabric and the lateral dimensions of individual mica flakes. However, no data on mica lengths is given in the paper to substantiate this. Examination of his photomicrographs (Potter 1968, plate 10) shows no marked variation in mica length for the samples pic-

tured. It is therefore suggested that the micas in these rocks did not show sufficient length variation to significantly affect the microfold wavelength.

Mineral proportions

No direct analysis of the effect of mineral proportions, such as the ratio of quartz to mica, on either microfold wavelength or cleavage spacing is attempted in this paper. However, a study of cleavages in psammitic rocks (Gray 1978) indicates that mineral proportions do influence microfolding in statistically homogeneous fabrics. Proportions of flaky minerals (e.g. micas) compared to the more rigid, less inequidimensional minerals (e.g. quartz and feldspar) appear to determine whether microfolding will occur. Poly-deformed psammites with the lowest proportions of flaky minerals (< 30%) do not contain microfolds associated with second generation or later cleavages (see fig. 16, *op. cit.*). In fact these develop rough cleavages instead of crenulation cleavages. The periodicity of the rough cleavages is generally dependent on the grain size of quartz and feldspar in the rock. It is suggested here that proportions of flaky minerals relative to other minerals will also influence the wavelength of the microfolds that develop.

Confinement distance

Confinement distance (cf. Biot 1964, fig. 1) is the thickness of a medium confined between two rigid layers. In this paper the term refers to the thickness of a micaceous or pelitic layer sandwiched between two quartzose or psammitic layers. Graphs of confinement distance (H) vs cleavage spacing (S) for three compositional layering fabrics (Fig. 7b–d) and one re-crenulated crenulation cleavage fabric (Fig. 7a) show a definite correlation between these parameters; correlation coefficients range from 0.79 to 0.99 with a mean of 0.91. Cleavage spacing, and therefore fold wavelength increases with increasing confinement distance. Potter (1968, fig. 5) has found similar relationships within deformed micaceous deposits from South Wales. This dependence of spacing upon confinement distance is however different for each sample. To a first approximation the correlation is linear, but the equation of each line of best-fit is different. They all have the general form:

$$S(\approx W_d) = m.\ H + b \qquad (2)$$

(where S = cleavage spacing, W_d = dominant wavelength, H = confinement distance, m = slope of line, and b = coefficient or line intercept), but different values of m and b. Obviously other parameters also influence the cleavage spacing. Graph e (Fig. 7) shows that cleavage spacing in particular layers will vary around larger mesoscopic folds. Spacing is much lower on the steeper limb with respect to the crenulation cleavage (i.e. sample points G, H, I, J and K) than on the corresponding flat limbs (i.e. sample points A, B, C, D, E, F, M, N, O, L, P, Q and R); this is reflected by a steeper slope of the best-fit line. It is clear that when mesoscopic folds develop in the confining layers, as illustrated in Fig. 7(d & f) and Fig. 13 (b & d), the cleavage spacing in the pelite is modified. This is most likely due to increased shortening across the fabric combined with angular shear (ψ) along the limbs associated with limb rotation of the microscopic folds. The original microfolds on these limbs become asymmetric and their long, steep limbs move closer together such that the cleavage spacing is reduced.

Grain size and mineral proportions are also probably responsible for some variations among the m and b coefficients of the graph. Fabrics with identical confinement distances but different grain sizes and/or mineral proportions will have different microfold wavelengths and therefore cleavage spacings. All of these factors interact to determine the microfold wavelengths in statistically homogeneous fabrics.

Layer thickness

In multilayer fabrics the layer thicknesses determine fold wavelengths. A ratio of competent layer thickness (t_1) to the incompetent layer thickness (t_2), that is the multilayer ratio, is used to provide a measure of layer spacing. Graphs of fold arc length (L) vs multilayer thickness ratio (t_1/t_2) for both lithological-layering multilayer fabrics (Fig. 8a) and differentiated S_1 layering multilayer fabrics (Fig. 8b) show distinct relationships

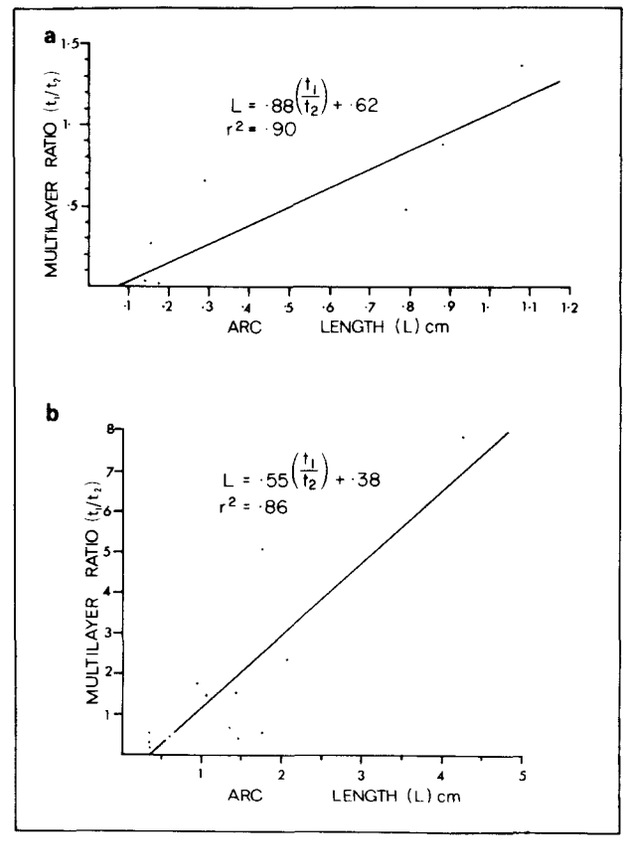

Fig. 8. Graphs of fold arc-length (L) vs the multilayer thickness ratio (t_1/t_2) in lithological layering fabrics (Graph a) and differentiated S_1 layering fabrics (Graph b). Measurements were taken from several samples to obtain a range of multilayer thickness ratios. Each point represents a mean of 30 – 50 cleavage spacing measurements.

between these parameters; correlation coefficients are 0.90 and 0.86 respectively. The arc lengths of microfolding in these fabrics will increase approximately linearly with increases in the multilayer ratio. The best-fit lines have the general form:

$$L = m\,(t_1/t_2) + b \qquad (3)$$

where L = fold arc length, t_1/t_2 = multilayer thickness ratio, and m and b are coefficients unique to each graph and therefore each fabric. These coefficients will vary depending on the contrast in rheological behaviour between the layers.

CLEAVAGE–FOLDING RELATIONSHIPS

Another important aspect of crenulation-folds, apart from the morphological characteristics previously described, is their relationship to crenulation cleavage. Features of the cleavage related to the folding, such as cleavage location, cleavage length, cleavage spacing and cleavage type, have particular implications about the mechanical significance of both the cleavage and the folding. Previous work on crenulation cleavage has not attempted to establish what parameters determine the location, the spacing and the length of these cleavages in the various pre-existing fabrics.

Cleavage location

The location of crenulation cleavages in crenulated rocks has both lithological and structural restrictions. Most commonly these cleavages are restricted to particular lithologies within deformed layered rock sequences (Fig. 13). The lithologies in which they occur have a distinct anisotropy, a feature which has long been recognized (cf. Knill 1960, Rickard 1961). Lithologies which have suitable anisotropy for crenulation cleavage development are (1) pelites which have a dimensional preferred orientation of flaky minerals, including bedding fabrics, slate fabrics (excluding the domainal types), schist fabrics, and psammites with well developed rough cleavage fabrics, and (2) laminated, or thinly bedded, multilayers including lithological layering fabrics, domainal slaty cleavage fabrics, pre-existing crenulation cleavage fabrics and thinly bedded psammites (see Gray 1977b, fig. 2). (1) and (2) correspond to statistically homogeneous and anisotropic multilayer fabrics respectively.

Mesoscopic structure in deformed layered rock sequences also controls crenulation cleavage locations. Variations in the style and intensity of structural elements, which have been superimposed on pre-existing lithological variations, commonly produce a complex distribution of crenulation cleavage. The structural controls are primarily related to mesoscopic folding where the cleavages are restricted to certain parts of the folds. Observed relationships include (1) restriction of the cleavage to the limbs of symmetric folds (Fig. 13b), (2) restriction of the cleavage to the steep limbs of asymmetric folds, that is those limbs which intersect the cleavage at the smallest angle (Fig. 13c & d), (3) restriction on the cleavage to the hinge zones (Fig. 13e), and (4) uniform occurrence and uneven spacing across the folds (Fig. 13f). Microscopic observations of zonal crenulation cleavages indicate that their location is dependent on the position of microfolds within the mesoscopic folds. Since the discrete types develop from the zonal types (Gray 1977b, 1979) it is suggested that the position of all crenulation cleavages are determined by the locations of microfolds in crenulated and mesoscopically folded fabrics. The described spatial variations in cleavage across mesoscopic folds reflect the distribution of strain both around and across the folds.

Cleavage length

Crenulation cleavages have finite length. Their lengths are variable and are commonly dependent on the confinement distance (H), that is the thickness of the pelitic layer in which they occur (see Fig. 13 a & c). Where the confinement distance is large, however, then

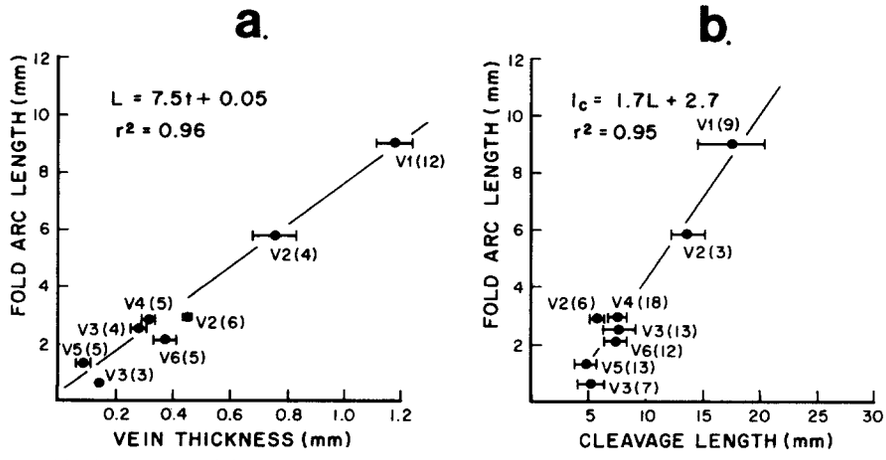

Fig. 9. (a) Graph of fold arc-lengths (L) vs vein thickness (t) for the buckled veins shown in Fig. 12. Each point represents a mean vein thickness with the standard deviation given by the bar. Number of measurements are given in brackets on the graph. (b) Graph of fold arc-length (L) vs cleavage length (l_c) for buckled veins and their associated discrete crenulation cleavages in the poly-deformed slate shown in Fig. 12. Numbers of the cleavage length measurements are shown in brackets on the graph.

the cleavages do not generally terminate against layer boundaries but are isolated within the pelitic layers. Parameters other than pelitic layer thickness must determine the cleavage lengths in this situation. Since both the discrete and zonal varieties of crenulation cleavage develop due to differentiation of microfolds (cf. Gray 1977b, 1979) then their length has to be determined by the extent of the microfolds. This is supported by the fact that the discrete types are nearly always transitional into microfolds at their terminations. Furthermore, in slates where discrete types are most common (Gray 1977b, fig. 3), there is microscopic evidence for a continuous transition from microfolds to zonal cleavages to discrete cleavages (Gray 1979, fig. 2). This implies that the length of discrete cleavages must be determined by the length of the microfolds parallel to their axial plane in profile section.

Cleavages associated with isolated buckled competent layers, such as quartz veins in pelite, show different relationships. These cleavages extend laterally from the limbs of the buckle folds into the matrix. Their lengths appear related to the buckles because the folds of large wavelength have the longest cleavages associated with them (see Fig. 12). Analysis of the folded veins in Fig. 12 (see Fig. 9b) shows a definite correlation ($r^2 = 0.95$) between length (1_c) and the fold arc length (L). It is suggested that the cleavage lengths define the extent of contact strain away from the folded veins. The contact strain perturbations were initially reflected by microfolds in the matrix which subsequently developed into crenulation cleavages. Analysis of the arc lengths (L) of the folded veins (Fig. 9a) shows that their arc length is dependent on the vein thickness (T), a feature which is characteristic of buckle folding (cf Biot 1957, Ramberg 1959, Sherwin & Chapple 1968). To a first approximation the relationship between cleavage length (1_c) and the arc length of the buckles (L) is given by:

$$1_c = 1.7L + 2.7 \quad (4)$$

The coefficients must reflect the competency contrast between the quartz veins and the pelite matrix.

Cleavage type

The type of crenulation cleavage, that is discrete or zonal, which develops in a crenulated fabric is apparently independent of crenulation-fold parameters. Graphs of fold shape, fold tightness, fold asymmetry and apparent percentage shortening crenulation cleavage type (see Gray 1977b, fig. 6) do not show distinct clusterings which would relate cleavage type to any particular fold parameter. Although folding is a necessary prerequisite for crenulation cleavage development the cleavage morphology is determined by other parameters, in particular the pre-existing fabric and the amount of solution-shortening (Gray 1977b). Since the discrete cleavage types develop from the zonal types with increased solution shortening then areas with discrete cleavage have undergone greater shortening than areas with zonal cleavages in the same rock. Variations in cleavage morphology firstly across mesoscopic folds, and secondly within individual fabrics, indicate strain inhomogeneity through these fabrics.

DISCUSSION

Folding theory, folding experiments and crenulation-folds

The geometric forms of folds are largely attributed to a combination of (1) the mechanical properties of the individual layers, (2) the degree of interlayer cohesion, and (3) the direction of the applied force responsible for folding with respect to the layering or anistropy. Four main types of folding have been recognized (cf. Hudleston 1973a):

1. *Buckling* (Ramberg 1963a)—where layer parallel loading of 'active' layers produces instabilities which may develop into folds
2. *Bending* (Ramberg 1963a)—where non-uniform forces act across either 'active' or 'passive' layering to produce folds
3. *Passive folding* (Donath 1963)—where forces act across 'passive' layering to produce folds
4. *Kinking* (Paterson & Weiss 1962)—where forces both parallel and oblique to well-developed layering produce folds with angular hinges and straight limbs which are confined to discrete zones although kinking is now considered to be a special form of buckling (Johnson 1970, 1977, Cobbold *et al.* 1971, Cosgrove 1976, Honea & Johnson 1976).

Aspects of these folding types are described and discussed by Ramberg (1963a), Ramsay (1967) and Hudleston (1973a, b). This discussion section relates the described characteristics of crenulation-folds with these defined types in an attempt to determine the mechanics of crenulation-fold development.

The geometrical analysis and the wavelength analysis of crenulation-folds have shown that the pre-existing fabric in crenulated rocks has not behaved in a truly passive manner during crenulation-fold development. Class 2 folds are supposed to indicate passive layer behaviour (Ramsay 1967, Hudleston 1973a, b). None of the crenulation-folds examined have exact similar (class 2) geometry but always consist of alternating class 1 and class 3 forms. The pre-existing anisotropy must play an active role in crenulation-folding because the type of anisotropy affects the morphology of the crenulation-folds which develop (see Fig. 2). Furthermore features of these fabrics such as thickness of pelitic layers (confinement distance), grain size of mica and the multilayer thickness ratio markedly influence crenulation fold wavelengths (see Figs. 6 & 9). Lack of microstructural evidence for significant movement along crenulation cleavages (Gray 1979) and the fact that all crenulation cleavages in rocks for which strain has been analysed thus far are subparallel (to within 4°) of the principal XY plane of the total bulk crenulation strain ellipsoid (Hara *et al.* 1968, Gray & Durney 1978, 1979a) both indicate that the once popular idea of a passive-slip fold (Donath & Parker 1964) origin for crenulation-folds is not really valid.

This restricts crenulation-folding to types 1 and 2 above where the layering plays an active role in the fold formation. This assumes though that kinking (type 4 above) is a buckling phenomenon. However, the wavelength relationships described previously, in particular the dependence of wavelength on competent layer thickness, mica length and confinement distance, are characteristic of buckling folds and not bending folds. Furthermore, bending folds are not as common as buckling types, and are predominantly associated with contact strain zones around (1) salt and magma diapirs, and (2) boudins, and pebbles in deformed conglomerates (cf. Ramberg 1963a). Analyses of deformed veins (Hara *et al.* 1968, p. 65) and poly-deformed porphyroblasts (Gray & Durney 1979a) in crenulation cleavage fabrics have shown that compression responsible for these crenulations must have been at a relatively low angle to the pre-existing anisotropy; and this implies a buckling deformation. The calculated strain distributed is incompatible with bending folds (cf. Ramberg 1963a, pp. 1–10).

Since most crenulation-folds are discontinuous, heterogeneously developed and often confined to particular lithologies (Fig. 13) they are geometrically 'internal' structures (see also Cosgrove 1972, 1976). This feature, combined with the dependence of wavelength upon confinement distance, is indicative of internal buckle folding (Biot 1963, 1964, 1965). The displacements accompanying this type of folding are restricted to a layer or zone of limited thickness. Crenulation-folds are therefore probably best described on the whole by internal buckling theory (self and rigid confinement respectively) rather than by unconfined buckling theory, which describes the buckling instability of a single layer or multilayer embedded in a relatively more ductile medium.

Internal buckling theory dictates that these folds are initiated as periodic instabilities within an anisotropic medium of 'infinite' or finite extent (Biot 1963). The anisotropy may be either (1) a homogeneous kind, for example, a statistically homogeneous slaty or schistose fabric, or (2) a layered kind consisting either of regularly alternating layers of differing viscosity, that is a regular multilayer, or of layers separated by planes of easy slip (Cobbold *et al.* 1971, pp. 25–26). For perfectly homogeneous fabrics a minimum wavelength compatible with the microstructure develops (Biot 1964, p. 567). This wavelength is therefore not only dependent on the confinement distance but also on the dimensions of the platy constituents (see section on crenulation-fold wavelengths; also Cobbold *et al.* 1971). This agrees well with the observations, firstly that crenulations in homogeneous geological materials are small scale structures and secondly that the minimum crenulation wavelength in slaty fabrics is generally lower than in schist fabrics. Such relationships are shown in Fig. 6 where it is clear that the length of mica in unconfined (i.e. the confinement distance is very much larger than the thickness of the flaky minerals) pelitic layers strongly influences crenulation-fold wavelength. The coefficients of equation (1), derived from Fig. 6 (a), must depend on other parameters, such as the thickness of the flaky minerals, the proportions of flaky to non-flaky minerals, and the amount of angular shear that the anisotropy has been subjected to (see section on crenulation-fold wavelengths). All these parameters determine the bending rigidity of the medium, that is the resistance of the medium to the vertical movement of the folding. Biot (1964, p. 563, equation 1) in a discussion of internal buckling within a laminated elastic medium under a plane stress, relates this bending rigidity to the factor $4M\xi^2$ in a threshold equation:

$$P = 4M\xi^2 + L(1-\xi^2)^2 \qquad (5)$$

where P = compression, $\xi = L/2H$, L = wavelength, H = confinement distance, and L and M are elastic coefficients of the medium. M is considered to represent the overall rigidity of the medium.

Wavelengths of internal buckle-folds in multilayer fabrics are dependent on confinement distance and the thickness of the competent layers. To a first approximation these relationships are expressed by:

$$W_d = 1.9\ (t_1 H)^{\frac{1}{2}} \text{ (Biot 1964, equation 20)} \qquad (6)$$

where W_d is the dominant wavelength (that is the wavelength initiated at the lowest stress if the system of layers are elastic or the wavelength of the component with the highest rate of amplification if the layers are viscous), t_1 the competent layer thickness, and H the confinement distance. This implies that the wavelength is independent of the material properties, such as elastic coefficients of the layers or their viscosity ratio. However, investigations of crenulation-fold wavelengths in two different multilayer fabrics (Fig. 9) where H was very large compared to the layer thickness, suggest that the layer properties have influenced the wavelengths of these folds. Wavelengths of folds developed in both a lithological layering and a differentiated S_1 layering are clearly dependent on the multilayer ratio (t_1/t_2). Each relationship is of the form expressed by equation (3) with different coefficients m and b. It suggested that these differences reflect the inherent differences of the original layering and its material properties.

Different orders of folding, that is folds with more than one characteristic wavelength, may develop due to either (1) the selective buckling of layers with different rheological properties (cf. Ramberg 1964), or (2) interference of buckling strains due to varying layer spacing, or layer thicknesses, within the multilayer (cf. Currie *et al.* 1962, Ramsay 1967, Durney 1968, Johnson & Ellen 1974).

One aspect which does not follow directly from the buckling theory itself is the finite development of fold shape, because the theory is concerned only with the initial sinusoidal deformations. However, model experiments simulating fold development in multilayers consisting of various materials (Ramberg 1961, Ghosh 1966, 1968, Johnson 1970, 1977, Cobbold *et al.* 1971, Honea & Johnson 1976) show complex variations in shape development. Various fold shapes, chiefly sinusoidal and kink-like, have been shown to develop out of initial, small amplitude, sinusoidal disturbances.

The reason for the appearance of kink forms is still a matter of debate (Johnson 1970, 1977, Cobbold *et al.* 1971, Honea & Johnson 1976, Cosgrove 1976). However, folding experiments in elastic multilayers (Honea & Johnson 1976) and folding theory (Johnson 1977, pp. 389–398) indicate that although the initial instability pattern is always sinusoidal, kink folds will develop when multilayers either (i) have finite contact shear strength between layers and are comprised of layers with nearly the same properties, or (ii) are very thick and have stiff and soft layers with comparable moduli. Sinusoidal and concentric-like folds develop when multilayers have either (i) low contact strength between layers, or (ii) very soft interbeds with high contact strengths.

The analysis of crenulation-fold shapes in this paper suggests that the most common low amplitude fold shape in statistically homogeneous slate and schist fabrics is sinusoidal. Sinusoidal, together with ellipsoidal shapes, are associated with the multilayers analysed. However, there is a tendency for kink-like and chevron-like folds to occur in psammite fabrics, a relationship dependent on the degree of development of rough cleavage (cf. Gray 1978). All these features obviously reflect the rheology of the pre-existing fabrics at low metamorphic grade. The multilayers have had either low contact strengths between layers or very high viscosity ratios between adjacent layers of high contact strength. The former is however more likely at these conditions.

Further implications from theory and experiment relate to fold axial-plane directions. Axial planes may either form approximately normal to loading or as a conjugate pair oblique to loading, depending on the previously defined (see equation 5) ratio of wavelength to confinement distance (Biot 1963, p. 322, Johnson 1970, Cobbold *et al.* 1971). They develop normal to loading under axial or oblique loading if ξ is small, producing harmonic symmetric or asymmetric folds respectively, while conjugate sets may arise if ξ is appreciable. Fabric parameters and the confinement distance therefore not only determine fold wavelength, but also the relationships of the axial planes to the developing fold-instabilities. It is interesting to note that the majority of crenulation-folds analyzed from southeastern Australia do not have conjugate axial plane cleavages. In terms of frequency of occurrence, conjugate structures are scarce. This indicates that the wavelengths of these natural crenulations, which are dependent on the fabric parameters, must generally be much smaller than the confinement distance, such that ξ is generally small. So-called conjugate cleavages have however been described by Knill (1960b) and Williams (1972).

Asymmetry, a common feature of crenulation folds has also been investigated experimentally (Ghosh 1966, Cobbold *et al.* 1971, Honea & Johnson 1976, Ramberg & Johnson 1976). It has been shown that asymmetrical folds result when the layering is oblique to the loading direction. Their development requires either simultaneous layer-parallel shearing and shortening, or layer-parallel shortening followed by shear (Johnson 1977, p. 397). Layer-parallel shear followed by shortening will not produce asymmetrical folds. Many asymmetrical crenulation-folds form as parasitic folds along the limbs of larger wavelength folds. Originally symmetrical, the crenulations develop asymmetry due to layer-parallel shear acting along the limbs of the larger folds as they develop. This development sequence has been verified experimentally by Ramberg (1963b, 1964).

SIGNIFICANCE OF CRENULATION-FOLDS

Crenulation-folds have important implications for cleavage development in crenulated rocks. These folds not only represent the initial disturbances, or strain perturbations, which are necessary for crenulation cleavage development, but they determine the location, the spacing and length of the cleavages in the fabric (see section on cleavage-folding relationships). The differentiation responsible for this variety of cleavage is intimately associated with the folding (cf. Cosgrove 1972, 1976, Gray 1976, 1979, Gray & Durney 1976, 1979b, Fletcher 1977b). The cleavages coincide with the limbs (zonal cleavage types) or the former limbs (discrete cleavage types) of the associated microfolds. Their development involves a redistribution of minerals across the microfolds, primarily solution-transfer of leucocratic minerals from microfold limbs to adjacent hinges at low grades of metamorphism. The limbs and hinges of folds in crenulated fabrics therefore represent potential sites of differentiation. A combination of other factors, stress and fabric related (cf. Gray & Durney 1979b) determine firstly whether differentiation will occur, and secondly whether a distinct cleavage will develop. In short, the folds associated with crenulation cleavages are a necessary pre-requisite for development of crenulation cleavages.

Crenulation-folds also play an important part in the

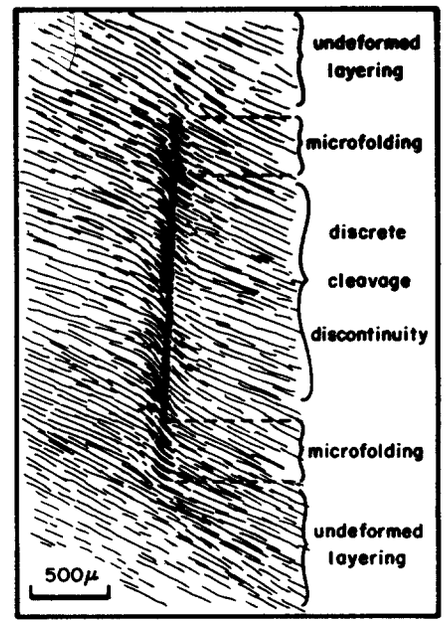

Fig. 10. Sketch of a discrete crenulation cleavage showing the strain perturbations within the host anisotropic fabric necessitated by development of the cleavage.

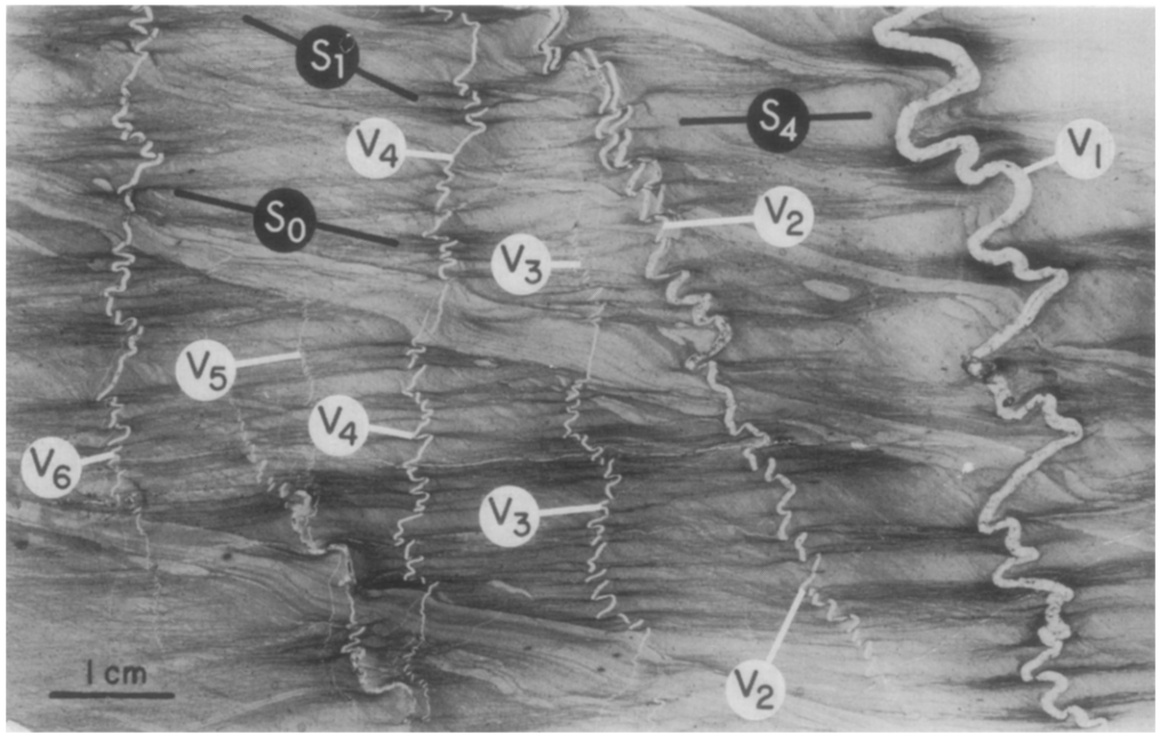

Fig. 12. Poly-deformed slate from the Silurian Chesleigh Formation, Sofala, N.S.W. Thin, cross-bedded, sandy interbeds delineate bedding (S_0). A slaty cleavage (S_1), developed within the pelite is crenulated and truncated by a sub-horizontal discrete crenulation cleavage (S_4). Buckled veins (sub-vertical) in the fabric have influenced the location, the spacing and length of the S_4 cleavages. Vein segments V_1 through V_6 show where measurements were obtained for the analyses depicted in Figs. 5 and 9. (Specimen by courtesy of M. J. Horden.)

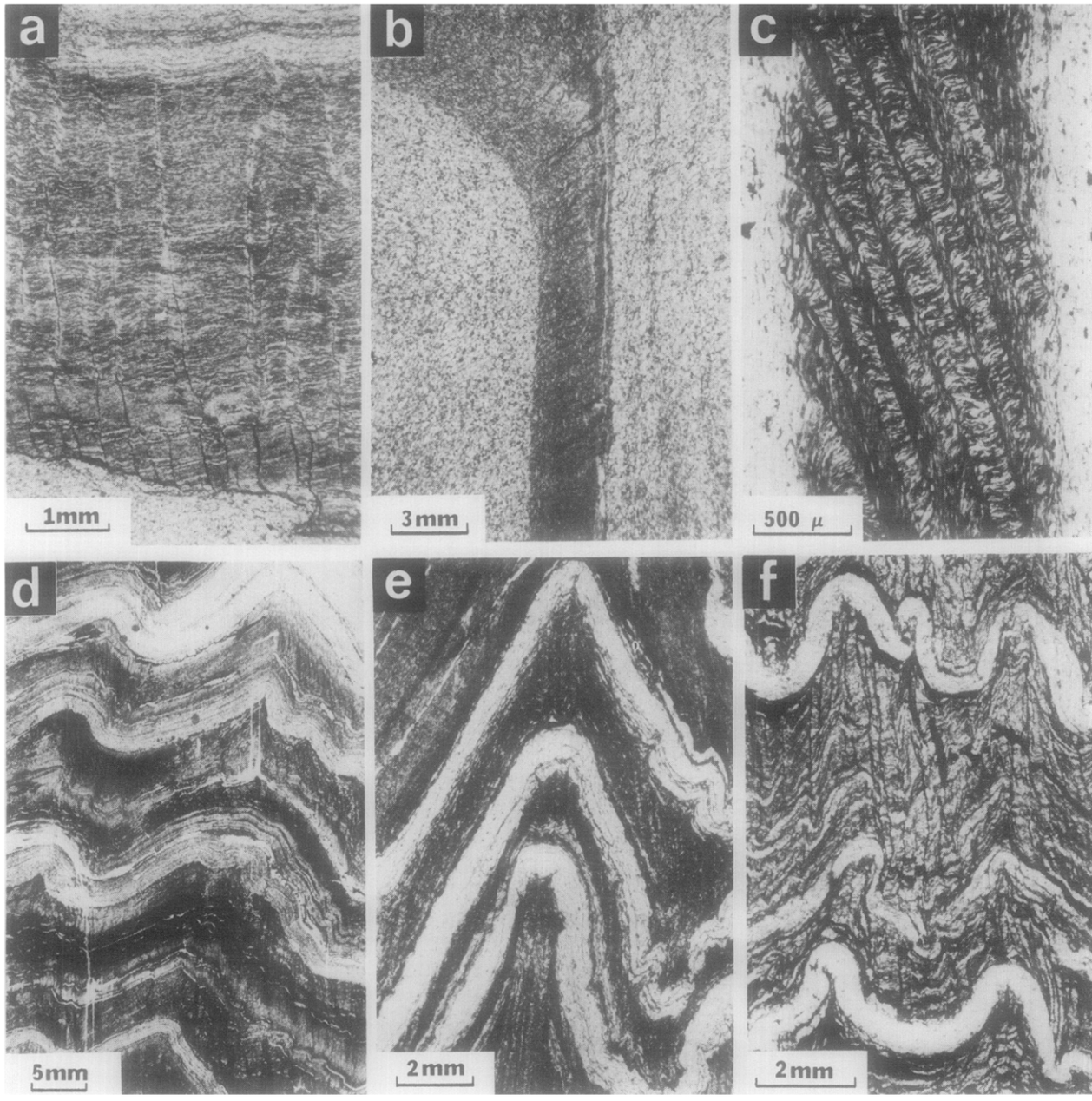

Fig. 13. Photomicrographs a, b and c illustrate the geometrically 'internal' nature of crenulation-folds and crenulation cleavages. d, e and f show various spatial relationships between crenulation cleavages and crenulation-folds. (a) Discrete crenulation cleavages and associated microfolds confined to a pelitic layer with a distinct slaty anisotropy. Bermagui, N.S.W. (b) Zonal crenulation cleavages developed in a pelitic layer with a bedding plane fabric. The cleavages occur along the limb of a larger asymmetric mesoscopic fold. Llandeilo, Wales. (c) Asymmetric microfolds and zonal crenulation cleavages confined to a pelitic layer along the larger mesoscopic folds. Gundagai, N.S.W. (d) Discrete crenulation cleavages developed in pelitic layers along the steeper limbs of asymmetric folds in a lithological layering fabric. Limerick, N.S.W. (e) Zonal crenulation cleavages in pelitic layers confined to the hinges of folds in a lithological layering fabric. Gundagai, N.S.W. (f) Unevenly spaced discrete crenulation cleavages in a pelite layer showing a relatively uniform occurrence across the fabric. Gundagai, N.S.W.

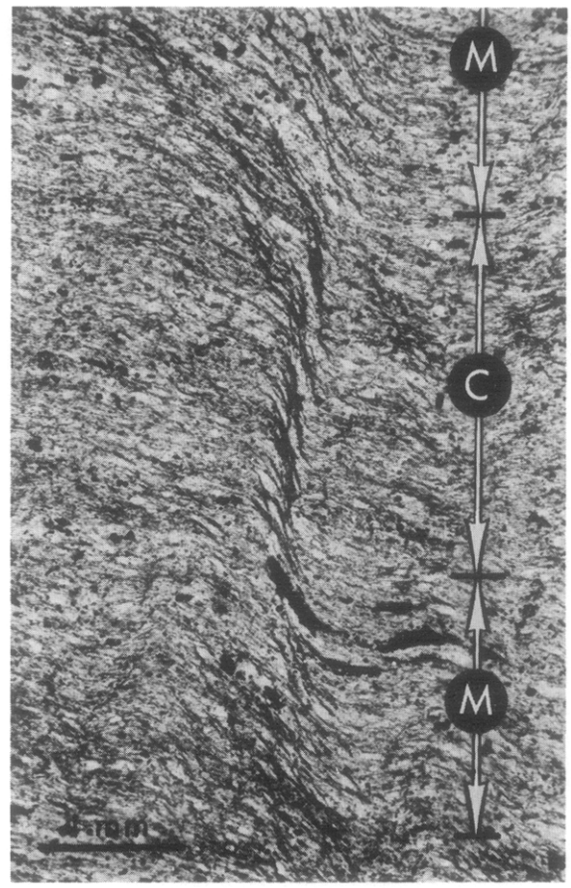

Fig. 14. Incipient crenulation cleavage (vertical) in a crenulated slate from Cooma, N.S.W. (MU. 10535). The cleavage (c) is a zone of accentuated echelon slaty cleavage traces which are coincident with the steep limb of an asymmetric microfold. This zone is transitional along its length into undifferentiated portions of the microfold(m).

propagation of crenulation cleavages. Crenulated fabrics with discrete cleavage types always show a transition from undifferentiated microfolds to zonal cleavages to discrete cleavages (e.g. Gray 1979, fig. 2). This transition is the result of increased differentiation, and therefore increased solution shortening, across individual microfolds. Because firstly there has been a volume reduction along these discrete cleavage discontinuities (cf. Gray 1979) and secondly because the rock is continuum, strain inhomogeneities must exist at their lengthwise terminations. This is reflected by the presence of microfolds there; i.e. discrete cleavages are transitional into microfolds at their lengthwise terminations (Fig. 14). The shortening due to the volume loss accompanying cleavage development is accommodated by micro-buckling of the host fabric anisotropy immediately adjacent to the cleavage terminations (see Fig. 10). It is suggested therefore that discrete crenulation cleavages propagate lengthwise due to a continual development, and subsequent differentiation, of microfolds ahead of the cleavage.

CONCLUSIONS

Crenulation-folds are initiated as buckling instabilities in stressed anisotropic materials. Their finite shape development is dependent on the degree of amplification and propagation (cf. Cobbold 1976), the confinement distance, the viscosity ratio of the multilayer or elastic moduli of the layers, layer thickness, grain size and proportion of flaky minerals, and the degree of associated cleavage development. The cleavage development is determined by the amount of crenulation strain and other stress fabric related parameters, which include grain shape, grain orientation, initial solubility of mineral phases, grain-boundary diffusion kinetics, nature of grain contacts and the microfold wavelengths (cf. Gray & Durney 1979a). Obviously the degree of cleavage development and the amplification and propagation of the associated folds, reflected by their interlimb angles, are interrelated because the latter markedly influences the differentiation process and therefore the degree of cleavage development (see Marlow & Etheridge 1977, fig. 8, Gray 1979, figs. 11 and 12). The buckling instabilities associated with propagating crenulation cleavages are of two types, each characterized by different wavelength-controlling parameters. These instabilities shown schematically in Fig. 11(a) are:

(1) *Type A Instability:* represented by internal buckle folds within a confined anisotropic medium (Figs. 11a(i), 7 (a–c), 14). This is the most common buckling instability associated with crenulation cleavages. The positions and extents of the micro-buckles (Type A instabilities) within the confined medium determine the location, spacing and length of the crenulation cleavages which develop. Because different orders of confinement exist in geological fabrics, for example the distances H_1 and H_2 in Fig. 11, internal buckle folds of different wavelengths may develop, as

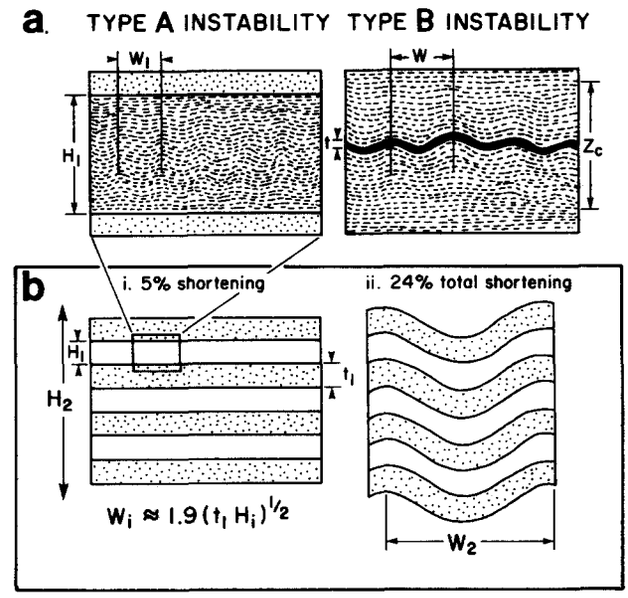

Fig. 11.(a) Schematic representation of the two main types of buckling instabilities associated with crenulation cleavage development. The instabilities are described in the text. (i) *Type A buckling instability:* Wavelengths (W_i) are dependent on confinement distance (H_i) and properties of the multilayer, such as thickness of the competent layer (t_1). (see equation in b). (ii) *Type B buckling instability:* Wavelengths (W) are dependent on competent layer thickness (t), the viscosity ratio between the layer and host (μ_1/μ_2), and the value of finite strain (S), given by:

$$W = 2\pi t\left(\frac{\mu_1}{6\mu_2}\cdot\frac{1}{3}\cdot\frac{S-1}{S^2}\right)^{1/3}$$ (Sherwin & Chapple, 1968, equation 6)

The zone of contact strain (Z_c) is given by:

$$Z_c = \frac{2}{\pi}W$$ (Ramberg 1960, P. 43)

(b) Sequence for the development of two orders of internal buckle folds (type A instability) in a confined lithological layering fabric subjected to a layer parallel compression.

shown by W_1 and W_2 respectively (see also Fig. 7d & e). Wavelengths of the early formed micro-buckles (W_1 in Fig. 11) will be modified during development of the larger wavelength folds (W_2). Their wavelengths will decrease and they will develop asymmetry along the W_2 fold limbs.

(ii) *Type B instability:* represented by contact strain inhomogeneities (buckle folds) adjacent to isolated, buckled, competent layers within an incompetent, anisotropic medium (Fig. 11a(i) & (ii)). These micro-buckles are initiated as strain perturbations, defined by the flow cells of Cobbold (1976, figs. 3 and 5), within the medium surrounding the buckled competent layer. They originate adjacent to the limbs of the folds in the competent layer and propagate lengthwise into the host medium. The extent of the contact strain, and therefore the micro-buckles, is dependent on the dominant wavelength of the buckled competent layer (cf. Ramberg 1960, p. 43). Clearly the positions, spacing and lengthwise extent of the associated crenulation cleavages must be dependent on the wavelengths and amplitudes of the buckles in the competent layer (see Figs. 9b, 13).

Acknowledgements — This paper was initiated from doctoral research work at Macquarie University, Sydney during the tenure of an Austra-

lian Government Postgraduate Research Award. Completion of the research and paper preparation was supported by a Departmental Research Allocation from the Department of Geological Sciences. VPI & SU.

The author would like to thank Dr. D. W. Durney for his stimulating ideas and guidance during the early part of the work, and Dr. P. J. Hudleston for his incisive comments on the manuscript. He also acknowledges the typing and drafting assistance provided by both Macquarie University and VPI & SU; thanks are extended to D. Oliver, R. Bashford, S. Knight, M. Eiss, G. Love, S. Dana for their respective services with drafting, photography and typing.

REFERENCES

Bayly, M. B. 1970. Viscosity and anisotropy estimates from measurements on chevron folds. *Tectonophysics* **9,** 459–474.

Bayly, M. B. 1971. Similar folds, buckling and great circle patterns. *J. Geol.* **79,** 110–18.

Bayly, M. B. 1974. An energy calculation concerning the roundness of folds. *Tectonophysics* **24,** 291–316.

Biot, M. A. 1957. Folding instability of a layered viscoelastic medium under compression. *Proc. R. Soc.* **A 242,** 444–454.

Biot, M. A. 1960. Instability of a continuously inhomogeneous viscoelastic half-space under initial stress. *J. Franklin Inst.* **270,** 190–201.

Biot, M. A. 1961. Theory of folding of stratified viscoelastic media and its implications in tectonics and orogenesis. *Bull. geol. Soc. Am.* **72,** 1595–1620.

Biot, M. A. 1963. Internal buckling under initial stress in finite elasticity. *Proc. R. Soc.* **A 273,** 306–328.

Biot, M. A. 1964. Theory of internal buckling of a confined multilayered structure. *Bull. geol. Soc. Am.* **75,** 563–568.

Biot, M. A. 1965. Further development of the theory of internal buckling of multilayers. *Bull. geol. Soc. Am.* **76,** 833–840.

Biot, M. A. 1967. Rheological stability with couple stresses and its application to geological folding. *Proc. R. Soc.* **A 298,** 402–423.

Campbell, J. D. 1951. Some aspects of rock folding by shear deformation. *Am. J. Sci.* **249,** 625–639.

Cobbold, P. R. 1975. Fold propagation in a single embedded layer. *Tectonophysics* **27,** 333–351.

Cobbold, P. R. 1976. Fold shapes as functions of progressive strain. In: *A discussion on natural strain and geological structure.* (edited by Ramsay, J. G. & Wood, D. S.) *Phil. Trans. R. Soc.* **A 283,** 129–138.

Cobbold, P. R. Cosgrove, J. W., & Summers, J. M. 1971. Development of internal structures in deformed anisotropic rocks. *Tectonophysics* **12,** 23–53.

Cosgrove, J. W. 1972. The interrelationship of microfolding and crenulation cleavage. Unpublished Ph.D. thesis, University London.

Cosgrove, J. W. 1976. The formation of crenulation cleavage. *J. geol. Soc. Lond.* **132,** 155–178.

Currie, J. B., Patnode, A. W. & Trump, R. P. 1962. Development of folds in sedimentary strata. *Bull. geol. Soc. Am.* **73,** 461–472.

Dale, T. N. 1892. On plicated cleavage foliation. *Am. J. Sci.* **43,** 317–319.

De Sitter, L. U. 1954. Schistosity and shear in micro- and macro-folds. *Geol. Mijnb.* **16,** 429–439.

De Sitter, L. U. 1956. *Structural Geology.* McGraw-Hill, New York.

Dieterich, J. H. 1970. Computer experiments on mechanics of finite amplitude folds. *Can. J. Earth Sci.* **7,** 467–476.

Donath, F. A. 1963. Fundamental problems in dynamic structural geology. in: *The Earth Sciences* (edited by Donelly, J. W.) Univ. Chicago Press, Chicago, 89–103.

Donath, F. A. & Parker, R. B. 1964. Folds and folding. *Bull. geol. Soc. Am.* **75,** 45–62.

Durney, D. W. 1968. Some experimental work in putty and plasticene. Unpublished M.Sc. thesis, University of London.

Durney, D. W. 1972. Solution transfer, an important geological deformation mechanism. *Nature, Lond.* **235,** 315–317.

Fletcher, R. C. 1974. Wavelength selection in the folding of a single layer with power-law rheology. *Am. J. Sci.* **271,** 1029–1043.

Fletcher, R. C. 1977a. Folding of a single viscous layer: Exact infitesimal-amplitude solution. *Tectonophysics* **39,** 593–606.

Fletcher, R. C. 1977b. Quantitative theory for metamorphic differentiation in development of crenulation cleavage. *Geology* **5,** 185–187.

Fletcher, R. C. & Sherwin, J. 1978. Arc lengths of single layer folds: A discussion of the comparison between theory and observation. *Am. J. Sci.* **278,** 1085–1098.

Fleuty, M. J. 1964. The description of folds. *Proc. geol. Ass.,* **75,** 461–492.

Flinn, D. 1962. On folding during three-dimensional progressive deformation. *J. geol. Soc. Lond.* **118,** 385–433.

Ghosh, S. K. 1966. Experimental tests of buckling folds in relation to strain ellipsoid in simple shear deformation. *Tectonophysics* **3,** 169–185.

Ghosh, S. K. 1968. Experiments of buckling of multilayers which permit interlayer gliding. *Tectonophysics* **6,** 207-249.

Gray, D. R. 1976. The origin and development of crenulation cleavages in low to medium grade metamorphic rocks from southeastern Australia. Unpublished Ph.D. thesis, Macquarie University, Sydney.

Gray, D. R. 1977a. Differentiation associated with discrete crenulation cleavages. *Lithos* **10,** 89–101.

Gray, D. R. 1977b. Some parameters which affect the morphology of crenulation cleavages. *J. Geol.* **85,** 763–780.

Gray, D. R. 1978. Cleavages in deformed psammitic rocks from southeastern Australia: Their nature and origin. *Bull. geol. Soc. Am.* **89,** 577–590.

Gray, D. R. 1979. Microstructure of crenulation cleavages: An indicator of cleavage origin. *Am. J. Sci.* **279,** 97–128.

Gray, D. R. & Durney, D. W. 1978. Relationship of crenulation cleavage to finite and incremental strain. (Abs.), *Geol. Soc. Am. Abs. Prog.* **10,** 411.

Gray, D. R. & Durney, D. W. 1979a. Investigations into the mechanical significance of crenulation cleavage. *Tectonophysics* **58,** 35–79.

Gray, D. R. & Durney, D. W. 1979b. Crenulation cleavage differentiation: Implications of solution-deposition processes. *J. Struct. Geol.* **1,** 73–80.

Hara, I., Uchibayashi, S. Yokota, Y., Uemura, H. & Oda, M. 1968. Geometry and internal structures of flexural folds. I. Folding of a single competent layer enclosed in a thick incompetent layer. *J. Sci. Hiroshima Univ.* **C6,** 51–113.

Heim, A. 1878. *Untersuchungen über den Mechanismus der Gebirgsbildung,* Vol. 2. B. Schwabe, Basel.

Hills, E. S. 1945. Examples of the interpretation of folding. *J. Geol.* **53,** 47–57.

Hobbs, B. E. 1971. The analysis of strain in folded layers. *Tectonophysics* **11,** 329–375.

Honea, E., & Johnson, A. M. 1976. A theory of concentric, kink and sinusoidal folding and of monoclinal flexuring of compressible elastic multilayers: IV. Development of sinusoidal and kink folds in multilayers confined by rigid boundaries. *Tectonophysics* **30,** 197–239.

Hudleston, P. J. 1973a. Fold morphology and some geometrical implications of theories of fold development. *Tectonophysics* **16,** 1–46.

Hudleston, P. J. 1973b. The analysis and interpretation of minor folds developed in the Moine rocks of Monar, Scotland. *Tectonophysics* **17,** 89–132.

Hudleston, P. J. 1973c. An analysis of "single-layer" folds developed experimentally in viscous media. *Tectonophysics* **16,** 189–214.

Hudleston, P. J. & Holst, T. B. 1977. Strain analysis in a buckle fold and its implications for the rheology of the layers during buckling. *Geol. Soc. Am. Abs. Prog.* **10,** 1029.

Johnson, A. M. 1970. *Physical Processes in Geology.* Freeman Cooper, San Francisco.

Johnson, A. M. 1977. *Styles of Folding.* Elsevier, Amsterdam.

Johnson, A. M. & Ellen, S. D. 1974. A theory of concentric, kink and sinusoidal folding and of monoclinal flexuring of compressible elastic multilayers. I. Introduction. *Tectonophysics* **21,** 301–339.

Knill, J. L. 1960a. A classification of cleavages with special references to the Craignish district of the Scottish Highlands. *Int. geol. Congr. XXI. Copenhagen* **18,** 317–325.

Knill, J. L. 1960b. The tectonic pattern in the Dalradian of the Craignish Kilmelfort district, Argyllshire. *J. geol. Soc. Lond.* **115,** 339–364.

Marlow, P. C. & Etheridge, M. A. 1977. The development of a layered crenulation cleavage in mica schists of the Kanmantoo Group near Macclesfield, South Australia. *Bull. geol. Soc. Am.* **88,** 873–882.

Mukhopadhyay, D. 1965. Effects of compression on concentric folds and mechanisms of similar folding. *J. geol. Soc. India* **6,** 27–41.

Paterson, M. S. & Weiss, L. E. 1962. Experimental folding in rocks. *Nature, Lond.* **195,** 1046–8.

Potter, J. F. 1968. Deformed micaceous deposits in the Downtownian of the Llandeilo region, South Wales. *Proc. geol. Ass.* **78,** 277–287.

Ramberg, H. 1960. Relationship between arc length and thickness of ptygmatically folded veins. *Am. J. Sci.* **258,** 36–46.

Ramberg, H. 1962. Contact strain and folding of a multilayered body under compression. *Geol. Rundsch.* **51,** 405–439.

Ramberg, H. 1963a. Strain distribution and the geometry of folds. *Bull. Inst. Geol. Univ. Upps.* **42,** 1–20.

Ramberg, H. 1963b. Evolution of drag folds. *Geol. Mag.* **100,** 97–106.

Ramberg, H. 1964. Selective buckling of composite layers with contrasted rheological properties: a theory for simultaneous formation of several orders of folds. *Tectonophysics* **1,** 307–341.

Ramberg, H. 1970. Folding of laterally compressed multilayers in the field of gravity: Part I. *Phys. Earth Planet. Inter.* **2,** 203–223.

Ramberg, I. B. & Johnson. A. M. 1976. A theory of concentric, kink and sinusoidal folding and of monoclinal flexuring of compressible elastic multilayers. V. Asymmetric folding in interbedded chert and shale of the Franciscan Complex, San Franscisco Bay area, California. *Tectonophysics* **32,** 295–320.

Ramsay, J. G. 1962. The geometry and mechanics of formation of "similar" type folds. *J. Geol.* **70,** 309–327.

Ramsay, J. G. 1967. *Folding and Fracturing of Rocks.* McGraw-Hill, New York.

Rickard, M. J. 1961. A note on cleavages in crenulated rocks. *Geol. Mag.* **98,** 324–332.

Rutland, R. W. R. 1976. Orogenic evolution of Australia. *Earth Sci. Rev.* **12,** 161–196.

Sherwin, J. & Chapple, W. M. 1968. Wavelengths of single layer folds: a comparison between theory and observation. *Am. J. Sci.* **266,** 167–179.

Shimamoto, T. & Hara, I. 1976. Geometry and strain distribution of single layer folds. *Tectonophysics* **30,** 1-34.

Williams, P. F. 1972. Development of metamorphic layering and cleavage in low grade metamorphic rocks at Bermagui, Australia. *Am. J. Sci.* **272,** 1–47.